

Bing Xu, Zhende Li, Shiyi Xie  
Information College  
Guangdong Ocean University  
China  
Jilin2013qx@126.com



**ABSTRACT:** In order to solve the problem of rotation invariant texture image retrieval, an image retrieval algorithm based on Log-Polar and nonsampled contourlet transform (NSCT) is proposed. Log-Polar transform was first applied to texture image to convert the rotation to translation. Then, translation invariant NSCT was employed to decompose the transformed images. Standard deviations, energies and entropies of the different directional subbands features were calculated to make up a 45-dimension feature vector. Finally, Canberra distance was used to compute the comparability of this feature vector to retrieval images. The experiment results showed that the proposed algorithm was able to obtain a higher recall rate.

## Categories and Subject Descriptors:

I.2.10 [Vision and Scene Understanding]: Video Analysis;  
I.4.10 [Image Representation]

## General Terms

Video Frame Processing, Content Processing

**Keywords:** Image Retrieval, Rotation Invariant, Log-Polar Transform, Nonsampled Contourlet Transform (NSCT)

**Received:** 29 June 2013, Revised 10 August 2013, Accepted 18 August 2013

## 1. Introduction

With the rapid development of information society, image data have been showing a trend of an exponential growth. Regular text search engines are almost helpless for image data [1], so how to retrieve desired images rapidly and accurately from a vast database has become a topical research issue [2] [3].

The texture in an image reflects the spatial distribution of gray level of the image, including the surface information of the image and the relationships between the image and its surroundings, thus achieving a better balance

between the macro information of the image and its micro-structure [4]. Texture in an image provides measurements of a region's regularity, roughness and smoothness. Texture analysis is an important means of image analysis, and has been widely used in object recognition, SAR image analysis, and content-based image retrieval and other fields [5] [6]. Literature [7] adopted wavelet transform to extract rotation invariant texture features, but with this algorithm, only approximate rotation invariant features could be obtained. literature [8] used a Log-Polar transform method to extract scale and rotation invariant texture features. However, this algorithm was not strong in texture enhancement. Literature [9] extracted rotation invariant features by direction/frequency decomposition. Despite its excellent performance, this algorithm was too complicated. Literature [10-11] made use of Hu moments to extract image rotation and scale invariant texture features. In this study, Lo-Polar transform and NSCT were adopted to extract rotation invariant texture features of texture images. The study also used Canberra distance to compute the comparability of the extracted image feature vector, and the experiment results proved the superiority of this method.

## 2. Log-Polar transform

Log-Polar transform is to transform an image from Cartesian Coordinates  $(x, y)$  to Polar coordinates  $(\gamma, \theta)$  first, then to Log coordinates  $(\rho, \theta)$ . The transform relationship is shown in the following equation [12].

Polar coordinates plane:

$$\begin{cases} \gamma = [(x - x_c)^2 + (y - y_c)^2]^{1/2} \\ \theta = \tan^{-1} \left( \frac{y - y_c}{x - x_c} \right) \end{cases} \quad (1)$$

where  $(x_c, y_c)$  is the center of the image in Cartesian Coordinates.

Log coordinates plane:

$$\begin{cases} \rho = \ln \gamma \\ \phi = \theta \end{cases} \quad (2)$$

The value range for  $\rho, \phi$  obtained directly from Equation (2) is too narrow and has decimal numbers. Assume the size of the image is  $512 \times 512$ , then the range of  $\rho$  and  $\theta$  would be  $[0, 6.2383]$  and  $[0, 2\pi]$ , respectively. In order to solve the problem, it is necessary to enlarge the image and undertake rounding operation by introducing parameter  $k_1, k_2$  as follows:

$$\begin{cases} \rho = k_1 \ln \gamma \\ \phi = k_2 \theta \end{cases} \quad (3)$$

Assume the size of the Log-Polar image is  $M \times N$  after the transform, and  $k_1, k_2$  is determined as follows: (4)

$$\begin{cases} N = k_1 \ln \gamma_{max} \\ \phi = k_2 2\pi \end{cases}$$

then

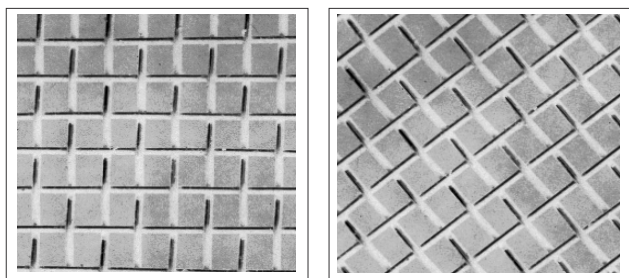
$$\begin{cases} k_1 = \frac{N}{\ln \gamma_{max}} \\ k_2 = \frac{M}{2\pi} \end{cases} \quad (5)$$

where  $\gamma_{max}$  is the radius of the maximum inscribed circle of the original image in Cartesian Coordinates.

When the image rotates, assume it rotates  $\beta$  degree relative to the center  $(x_c, y_c)$  then

$$\phi_1 = k_2(\theta + \beta) = \phi + k_2 \beta \quad (6)$$

When the image rotates, its Log-Polar image translates along  $\phi$  axis. Figure 1(a) is a sample texture image, and Figure 1(b) is the image of Figure 1(a) when the latter rotates  $40^\circ$ . Figure 2 are corresponding images of the two in Figure 1 after Log-Polar transform is applied to them. As shown in Figure 2, the image in Figure 2(b) is obtained when the image in Figure 2(a) translates vertically.



(a) Sample image (b) Image after 1(a) rotates  $40^\circ$

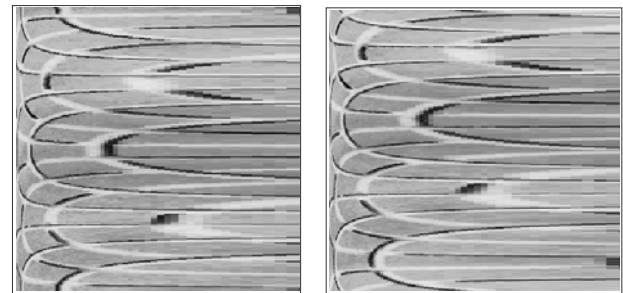
Figure 1. Two Sample Images

### 3. Nonsubsampled Contourlet Transform

Contourlet transform has the multi-resolution and local time-frequency analysis features that wavelet transform presents, as well as directionality and anisotropic features that wavelet transform lacks [13]. It is, therefore, a superior image presentation method, and has been widely applied

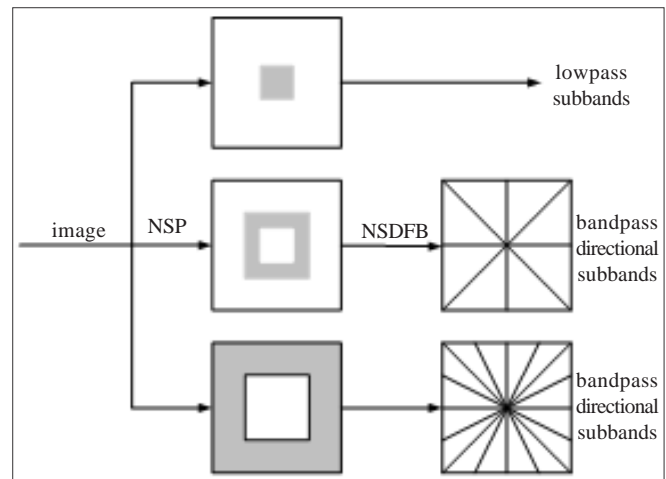
in many image processing technologies. However, in both Laplace decomposition and directional filtering, there are upsampling and subsampling operations, so translation invariance is not a feature in Contourlet transform.

In order for Contourlet transform to be translation invariant, Cunhua proposed a nonsubsampled Contourlet transform [14]. NSCT removes the subsampling sections in two-level implementations of Contourlet transform and is made up of Nonsubsampled Pyramid (NSP) and Nonsubsampled Directional Filter Bank (NSDFB) (See Figure 3). Therefore, it is translation invariant [15].

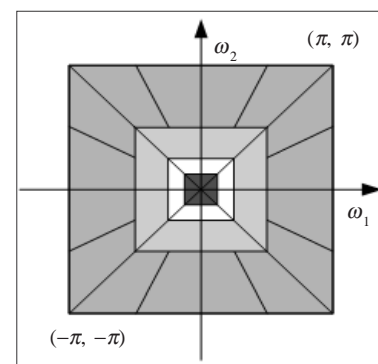


(a) Log-Polar transform image of 1(a) (b) Log-Polar transform image of 1(b)

Figure 2. Log-Polar Transform Image of Figure 1



(a) Multi-scale partitioning structure

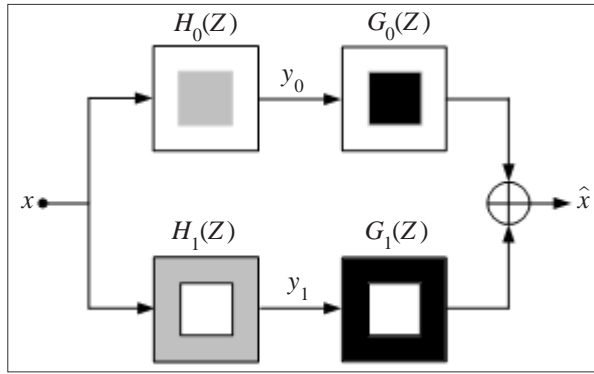


(b) Frequency partitioning

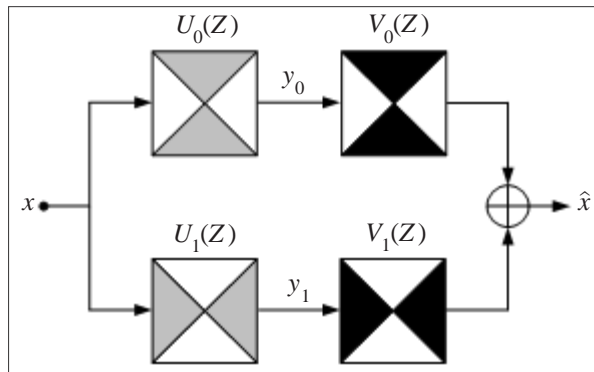
Figure 3. Multi-scale and Frequency Partitionings of Nonsubsampled Concourlet

The two-channel nonsubsampled filter adopted is as

shown in Figure 4:



(a) Nonsubsampled Pyramid Filter Bank



(b) Nonsubsampled Directional Filter Bank

Figure 4. Nonsubsampled Filter Bank

As both Nonsubsampled Pyramid Filter Bank and Nonsubsampled Directional Filter Bank satisfy the Bezout identity.

$$U_0(Z) V_0(Z) + U_1(Z) V_1(Z) = 1 \quad (7)$$

$$H_0(Z) G_0(Z) + H_1(Z) G_1(Z) = 1 \quad (8)$$

Therefore, NSCT can be completely reconstructed [15]. NSCT has the following three strengths: (1) It is translation invariant, and the scales between and the sizes of subbands images are identical; (2) It has higher redundancy with more complete information for each subbands image; (3) According to nonsampling theory, NSCF's low frequency subbands will not have frequency confusion, and is more directional.

With these advantages, NSCF is suitable for extracting geometric features of images. In this paper, NSCF and Log-Polar transform are combined in rotation invariance image retrieval.

#### 4. Rotation Invariant Texture Image Retrieval

When an image rotates, its Log-Polar image translates. In this paper, Log-Polar transform of the rotated image will be outlined first, followed by the discussion about extraction of image texture features using NSCF's translational invariance, and the use of Canberra distance

to compare the similarities between this image and the image library.

#### 4.1 Extraction of Texture Features

The procedures for extracting texture features were as follows:

(1) For a class of texture images, the average energies of different rotation angles were different, so it was necessary to normalize the energy of each texture image.

$$f(x, y) \leftarrow \frac{f(x, y)}{\frac{1}{N^2} \sum_{x=0}^{N-1} \sum_{y=0}^{N-1} f^2(x, y)^{1/2}} \quad (9)$$

(2) Log-Polar transform was applied to the images with normalized energies, converting image rotation and scale transform into translation of Log-Polar transformed images or keeping the visual information relatively unchanged. In the experiment,  $S = R = 360$  was chosen to ensure that the sizes of the Log-Polar images were identical after rotation and scale transform was applied to them.

(3) NSCF translational invariance was adopted to remove the effect of Log-Polar image translation so as to obtain rotation and scale-invariant texture features. Fifteen directional subbands including lowpass subbands were obtained after a three-level NSCF decomposition of Log-Polar images

(4) Standard deviations, energies and entropies for each directional subband were calculated as shown in the following three equations.

$$f_1(k) = \sqrt{\frac{1}{N \times N} \left( \sum_{i=1}^N \sum_{j=1}^N I_k(i, j) - u_k \right)^2} \quad (10)$$

$$f_2(k) = \frac{1}{N \times N} \sum_{i=1}^N \sum_{j=1}^N |I_k(i, j)| \quad (11)$$

$$f_3(k) = \sum_{i=1}^N \sum_{j=1}^N I_k(i, j) \log I_k(i, j) \quad (12)$$

Where  $I_k(i, j)$  is coefficient of the  $k^{\text{th}}$  subbands,  $u_k$  is the average value of  $I_k(i, j)$ , and  $k = 1, \dots, 15$ . The 45-dimension feature vector was obtained by combining the above three features.

$$f = [f_1(1) \dots f_1(15), f_2(1) \dots f_2(15), f_3(1) \dots f_3(15)] \quad (13)$$

#### 4.2 Comparability measure

Significant differences existed among individual features, and using Euclidean distance was likely to cover up the role of the small eigenvalues and fail to achieve the desired effect, so in this study, Canberra distance was selected for computing comparability. Let  $f_q$  be the query image feature vector, and  $f_d^j$  the feature vector of the  $j^{\text{th}}$  image in the image library. The distance was defined as [16]:

$$d_c(j) = \sum_{i=1}^l \frac{|f_q(i) - f_d^j(i)|}{|f_q(i) + f_d^j(i)|} \quad (14)$$

In the equation,  $f_q(i)$  is the  $i^{\text{th}}$  eigenvalue of the query image,  $f_d^j(i)$  the  $j^{\text{th}}$  eigenvalue of the  $i^{\text{th}}$  image in the image library, and  $l$  the length of feature vectors. Let  $M$  be the number of images in the image library, and after  $d_c(i), j = 1, \dots, M$  is obtained, if to all  $j (j \neq n)$ , the inequality (15) holds, then it is determined that the query image belongs to class  $n$ .

$$d_c(n) < d_c(j) \quad (15)$$

## 5. Experimental Evaluation

Brodatz texture database is an image database built by University of Queensland, Australia where images are classified. It is suitable for texture feature extraction, texture categorization and texture segmentation. The experiment in this study was conducted with Brodatz's rotation texture image library which held 91 pictures of  $512 \times 512$ , classified into 13 classes with seven in each class. One of the images in each class was original, and other six were rotation images of the original, with rotation angles as 30, 60, 90, 120, 150 and 200, respectively [17]. Figure 5 shows the 13 original images in the library.

Recall rate was taken as the evaluation index, and its definition was:

$$\text{recall} = \frac{\text{number of right pictures recalled}}{\text{number of pictures recalled}} \times 100\% \quad (16)$$

The average recall rate of an image library is the average of recall rates of all images in the library.

In order to verify the effectiveness of algorithm proposed in this study, a comparison was made between the algorithms based on DT-CWT method [17], Log-Polar and DT-CWT[18], and Radon and wavelet transform [19]. Table 1 presents the comparison of recall performance of these four algorithms.

Table 1 indicates that the recall based on Log-Polar and DT-CWT was higher than that based on DT-CWT by 1.73%, the recall based on Radon and wavelet transform, which was 95.8%, was between the above two methods. The algorithm based on DC-CWT performed FFT with the feature matrix respectively after the images underwent DT-CWT transform so as to eliminate the impact of

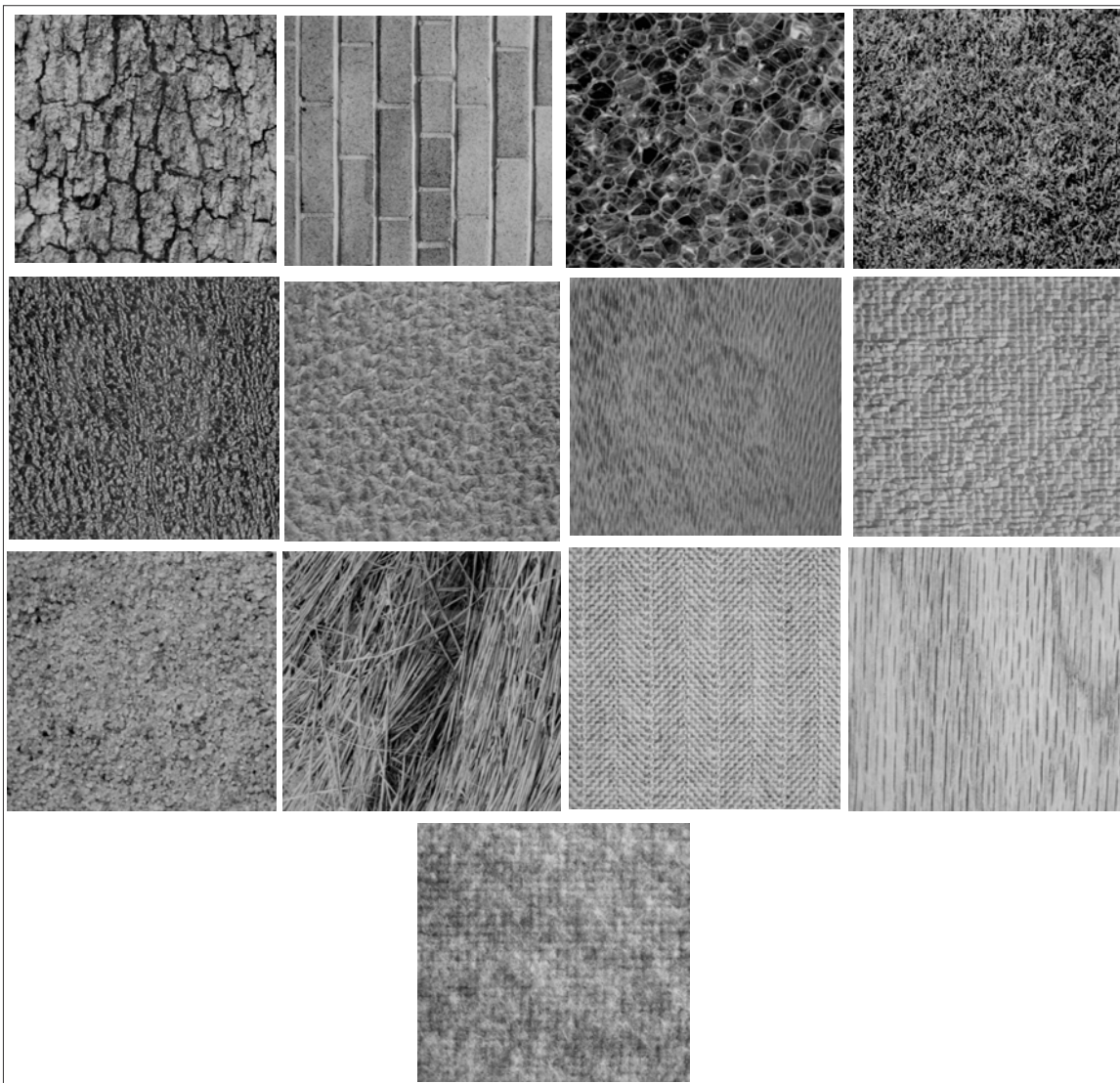


Figure 5. Originals of Images in Brodatz Image Library

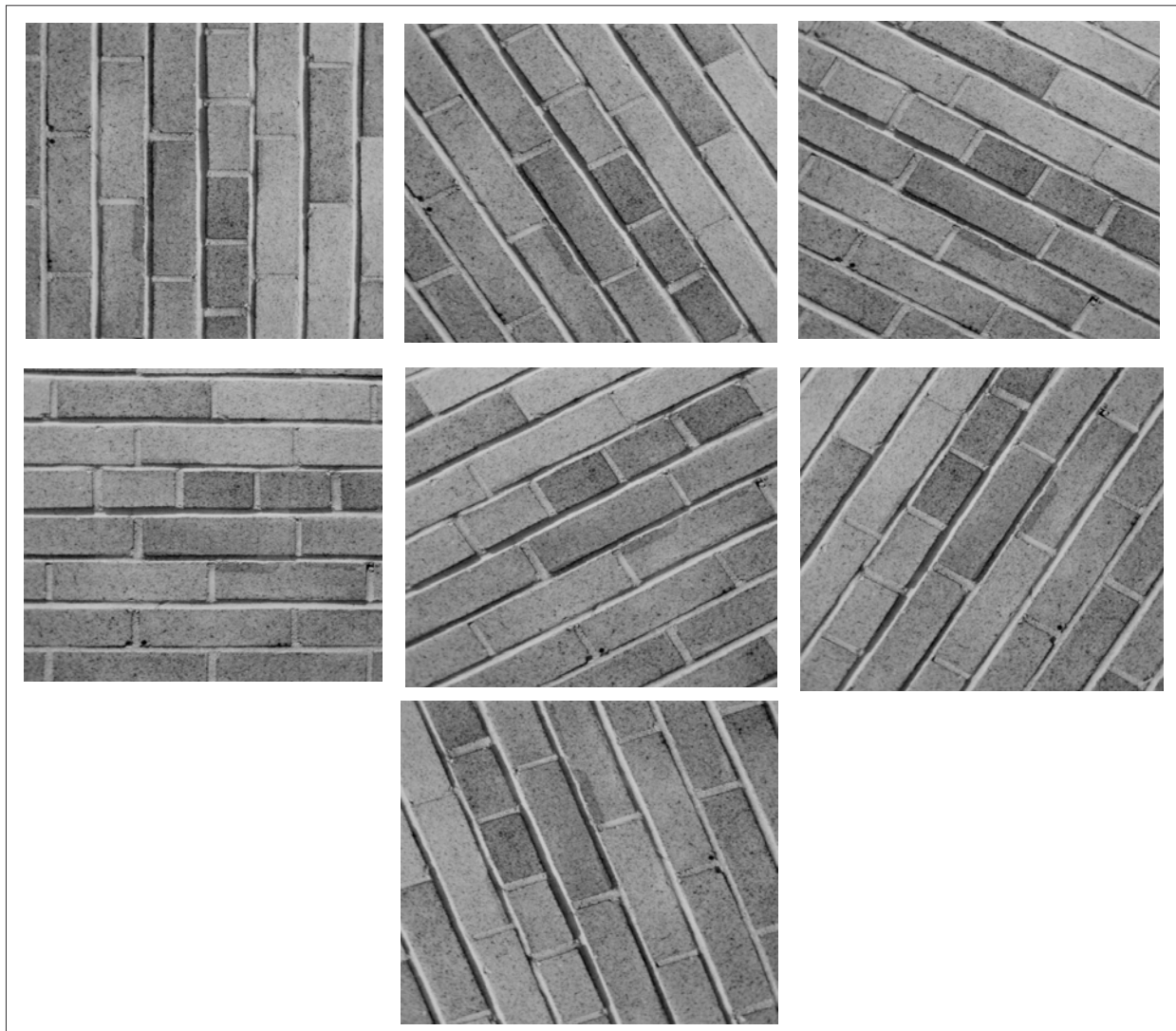


Figure 6. Images at Different Rotation Angles

Method	Recall (%)
Based on DT-CWT[17]	94.89
Based on Log-Polar and DT-CWT[18]	96.62
Based on Radon and wavelet transform[19]	95.87
Used in this study	98.45

Table 1. Comparison of Four Algorithm Recall Performance

translation. With the method based on Log-Polar and DT-CWT, Log-Polar transform of the images was applied firstly, converting rotation to translation, and then DT-CWT translation invariance was re-used to extract rotation invariant texture features. Like the method based on Log-Polar and DT-CWT, the first step of the method proposed in this paper made use of Log-Polar transform to turn the image rotation into translation. Then NSCT's translation invariance as well as its excellent capacity to enhance texture feature was employed to extract rotation invariance texture features, and the recall obtained was 98.45%.

## 5. Conclusion

Log-Polar transform can convert image rotation to translation. Nonsubsampled Contourlet Transform is characterized with good translational invariance and the capacity to enhance texture features. This paper proposes an image rotation invariance recall algorithm based on Log-Polar and Nonsubsampled Contourlet Transform. This method effectively integrates the advantages of both Log-Polar transform and Nonsubsampled Contourlet Transform by first converting image rotation variance to translational

variance with Log-Polar transform, and then extracting image rotation invariance texture features with Nonsubsample Contourlet transform. The study's results indicate that the proposed method has a superior performance in image recall.

## 6. Acknowledgements

This work was financially supported by 2013 Dr. research programme fund of personnel department, Guangdong Ocean University.

## References

- [1] Pun, Chi-man., Lee, Moon-Chun. (2003). Log-polar wavelet energy signatures for rotation and scale invariant texture classification. *IEEE Transactions on Pattern Analysis and Machine Intelligence*, 25 (5) 590-603.
- [2] Kourosh, J. K., Hamid, S. Z. (2005). Rotation-invariant multi-resolution texture analysis using radon and wavelet transform. *IEEE Trans on Image Process*, 14 (6) 783-794.
- [3] Cuip, C., Li, J. H., Zhang, H. C. (2006). Rotation and scaling invariant texture classification based on radon transform and multi scale analysis. *Pattern Recognition Letters*, 27, p. 408- 413.
- [4] Sastry, C. S., Arun, K., Pujari, B. L, et al. (2004). A wavelet based multi resolution algorithm for rotation invariant feature extraction. *Pattern Recognition Letters*, 25:1845-1855.
- [5] Sim, D. G., Kin, H. K., Park, R. H. (2004). Invariant texture retrieval using modified Zernike moments. *Image and Vision Computing*, 22, p. 331-342.
- [6] Kingsbury, N. (2001). Complex wavelets for shift invariant analysis and filtering of signals. *Applied and Computational Harmonic Analysis*, 10, p. 234-253.
- [7] Yang, Ruihong., Pan, Quan., Chen, Yong-mei. (2005). Application of invariant wavelet moment to image recognition. *Computer Applications*, 11 (6) 239-241. (In Chinese)
- [8] Jiang, Jin-shan., Yu, Ying-lin. (2004). Realization of the texture classification of invariant scale and rotation by support vector machines. *Journal of South China University of Technology* (Natural Science Edition), 32 (5) 26-33. (In Chinese)
- [9] Han, Guang., Zhao, Chun-xia. (2010). Rotation invariant texture classification based on orientation frequency decomposition. *Acta Photonica Sinica*, 39 (2) 352-356. (In Chinese)
- [10] Liu, Jin., Zhang, Tianxu. (2004). The generalization of moment invariants. *Chinese Journal of Computers*, 27 (5) 668-674. (In Chinese)
- [11] Wang, Yiping., Huang, Xinsheng., Li, Xiaolei . (2008). Moment invariants of gray distorted based on Hu moments. *Journal of Dalian Maritime University*. 34 (4) 23-27. (In Chinese)
- [12] Li, Liulin., Shen, Haibin. (2009). Robust feature extraction arithmetic based on parametrical log-polar transformation for texture image. *Journal of Zhejiang University (Science Edition)*, 36 (2) 162-164. (In Chinese)
- [13] Lian, Xueqiang . (2008). Research of nonsubsampling contourlet transform and its application on image processing. Xiamen University. (In Chinese)
- [14] Cunhua, A. L., Jiang Zhou, N., Minh. Do. (2006). The nonsubsampling counourlet transform theory, design, and applications. *IEEE Trans. on Image Processing*, 15 (10) 3089-3101.
- [15] Chen, Xiaolin., Wang, Yanjie. (2011). Infrared and visible image fusion based on nonsubsampling contourlet transform. *Chinese Optics*, 4 (5) 489-495. (In Chinese)
- [16] Hao, Yubao., Wang, Renli ., Gu, Lijuan. (2010). A new image retrieval method using contourlet-based rotation invariant feature for remote sensing images. *Journal of Image and Graphics*, 15 (4) 670-676. (In Chinese)
- [17] Wang, Chengru., Luo, Xiaoyan. (2007). Image retrieval with scale and rotation invariant texture features. *Electronic Measurement Technology*, 30 (5) 29-31. (In Chinese)
- [18] Shang, Yan., Liang, Qiusheng (2007). Rotation invariant texture classification algorithm based on Log-Polar and DT-CWT. *Computer Engineering and Applications*, 43 (11) 48-50. (In Chinese)
- [19] An, Zhiyong., Wang, Xiaohua., Zhao, Shan (2007). Content-based image retrieval based on radon and wavelet transform. *Journal of Xidian University*, 34 (3) 409-413. (In Chinese)